

Growth of GaN Nanotubes and Nanowires on Au–Ni Catalysts

N. V. Sibirev^{a,b*}, H. Huang^c, E. V. Ubyivovk^{a,b}, R. Lv^c, D. Zhao^c, Q. Guang^c,
Yu. S. Berdnikov^b, X. Yan^d, A. A. Koryakin^b, and I. V. Shtrom^{a,e}

^a St. Petersburg State University, St. Petersburg, 199034 Russia

^b St. Petersburg National University of Information Technology, Mechanics, and Optics (ITMO University),
St. Petersburg, 197101 Russia

^c Dalian University of Technology, Dalian, 116024 China

^d Beijing University of Posts and Telecommunications, Beijing, 100876 China

^e Institute for Analytical Instrumentation, Russian Academy of Sciences, St. Petersburg, 198095 Russia

*e-mail: sibirev@mail.ioffe.ru

Received November 27, 2018; revised November 27, 2018; accepted November 28, 2018

Abstract—Arrays of GaN nanowires (NWs) and nanotubes (NTs) have been grown by metalorganic vapor phase epitaxy using a gold–nickel film as the catalyst. The simultaneous formation of both NTs and NWs in one process in the presence of various Au–Ni catalyst compositions is explained. It is established that NTs grow on solid catalyst particles, while NWs grow according to the classical vapor–liquid–solid mechanism. The optoelectronic properties of obtained NTs and NWs have been studied using photo- and cathodoluminescence techniques.

DOI: 10.1134/S1063785019020329

Solid solutions of group-III nitrides provide a basis for fabricating light-emitting diodes (LEDs) and light-absorbing devices operating in a broad spectral range including both visible and UV wavelength intervals [1, 2]. Special features of the geometry of nanocrystalline wires (NWs) and nanotubes (NTs) allow the integration of materials with significantly different lattice parameters to be integrated—in particular, semiconducting nitrides and silicon [2–5]. These properties account for the increasing interest in studying processes involved in the formation of NWs and NTs [2, 4–7].

In our experiments, arrays of gallium nitride (GaN) NWs and NTs have been grown by metalorganic vapor phase epitaxy in a horizontal reactor with cooled walls. First, a sapphire substrate was covered with a 3- μm -thick GaN sublayer; 2-nm-thick Ni and 2-nm-thick Au deposits were then formed by magnetron sputtering. Then, the deposited film was annealed for 10 s at 850°C so as to form Au–Ni catalyst particles, after which the substrate was cooled to 750°C and the flows of gallium and nitrogen precursors (2 sccm trimethylgallium and 40 sccm ammonia, respectively) were switched on. The growth process was described in more detail elsewhere [7].

As-grown samples with GaN NWs arrays were studied by measuring their cathodoluminescence (CL) and photoluminescence (PL) spectra, which are presented in Fig. 1. The PL spectra were mea-

sured at 10 K under excitation with He–Cd laser radiation ($\lambda = 325$ nm). The PL spectrum in Fig. 1 displays three clearly pronounced emission bands I_A (3.47 eV), I_B (3.44 eV), and I_C (3.27 eV). The I_A and I_C bands are well known for bulk GaN [1, 8], where I_A peak corresponds to excitons bound on neutral donors [1, 6, 8] and I_C peak can be related to donor–acceptor pairs [1, 8] and/or inclusions of metastable cubic phase (β -GaN) in NWs [1, 2]. The band of emission at 3.44 eV (I_B peak) has been observed for GaN NWs grown with Ni catalyst and can be explained by the appearance of bound exciton on a neutral acceptor [9]. Possible acceptors are Ni, Ga vacancy, or C [8].

The CL spectra were measured for single NWs with the aid of a Gatan MonoCL3+ setup. The signal intensity (brightness) for various nanostructures could exhibit 200-fold differences (Fig. 1b). Both bright and dim structures have been studied by transmission electron microscopy (TEM) on a Carl Zeiss Libra 200FE microscope and the typical results are presented in Fig. 2. As can be seen, bright NWs contain inner cavities—that is, represent NTs rather than true NWs. Detailed analysis of the TEM images of NTs revealed catalyst nanoparticles occurring inside the NTs (Fig. 2d). In addition, the composition of these internal nanoparticles was studied by local energy-dispersive X-ray (EDX) spectroscopy. The Ni/Au ratio of catalyst materials in the particles occurring inside NTs

significantly differs from the initial film composition, in which the content of Au and Ni was approximately equal. In contrast, the particles occurring inside NTs, were strongly enriched with Ni. The Ni/Au ratio measured in these particles varies from 3 to 9. This circumstance allows us to suggest that the compositions of catalysts on which NWs and NTs grew were different.

The annealing of a gold–nickel film even at lower temperatures leads to active mutual diffusion of Ni and Au atoms [10]. Since the diffusion of Ni atoms in Au is much faster than that of the inverse process, the film exhibits separation [10]. The phase diagram of the Au–Ni system contains the region of immiscibility with a critical point at 810.3°C corresponding to 71% Ni–29% Au [10, 11]. The annealing temperature used in this work was above this point, but the clusterization of Au–Ni films also took place above the indicated critical value [10] while the growth of NWs and NTs proceeded at lower temperatures. As a result, a small fraction of islands formed during annealing and subsequent cooling of the film must be enriched with Ni (>75% Ni), while the majority of islands must contain >50% Au. The study of catalyst nanoparticles found at the ends of NWs and NTs (occurring inside NTs and on the film surface) confirmed this assumption. All nanoparticles occurring inside NTs had Ni/Au ratios above 3. Most nanoparticles occurring on the substrate had relatively small nickel content with Ni/Au < 1. At the NW top, both Au-rich particles (Ni/Au < 1) and Ni-rich particles (Ni/Au > 3) could be observed. Nickel particles interacting with GaN form solid Ni–Ga phases [6, 7, 12, 13]. In contrast, gold dissolves in Ga at temperatures above 750°C [3, 11] and forms droplets [3].

The formation of liquid catalyst droplets leads to NW growth according to the well-known vapor–liquid–solid (VLS) mechanism [3, 5, 12, 14]. Since the droplet permanently wets the NW top face, internal cavities cannot form and, hence, continuous NWs grow. The growth on solid catalyst particles can also lead to the formation of NWs, but only via the vapor–solid–solid (VSS) mechanism [12, 13]. Since the diffusion in this case proceeds only on the crystal surface [5, 6] rather than over the entire catalyst surface, NTs can form instead of NWs [5] because gallium and nitrogen fluxes on the surface can rapidly decrease from the edge to center.

For the growth of NWs or NTs according to the VSS mechanism, it is usually assumed that the NW (or NT) diameter is approximately equal to the diameter of the catalyst particle [3, 14]. In this work, the catalyst particles found after growth termination had diameters about 40 nm, while the external diameter of NTs amounted to 100 nm and their internal diameter was about 30 nm. This probably implies that catalyst parti-

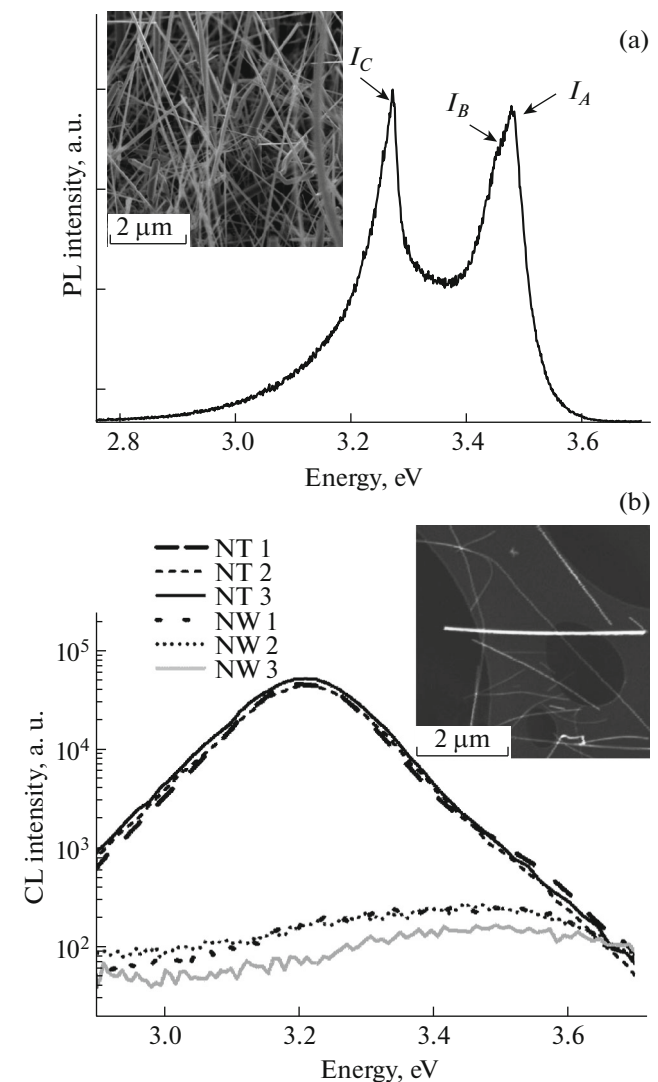


Fig. 1. (a) PL spectrum of GaN NW array; the inset shows a scanning electron microscopy image of this object; (b) CL spectra of various single GaN NTs and GaN NWs; the inset shows these objects as imaged by scanning tunneling microscopy.

cles during growth contained excess Ga that incorporated into NTs on cooling. During growth, a solid nickel particle was covered by a layer of liquid gallium by analogy with a solid particle in the catalyst droplet observed in situ in IBM experiments [14]. In some cases we observed several nanoparticles occurring inside NTs (Fig. 2c), which implies that a catalyst particle could contain several solid nanoparticles during growth.

In concluding, this work demonstrated the possibility of simultaneous formation of both GaN NTs and NWs in one growth cycle. This phenomenon has been explained by NT formation on solid catalyst particles and NW growth from liquid droplets. The PL and CL

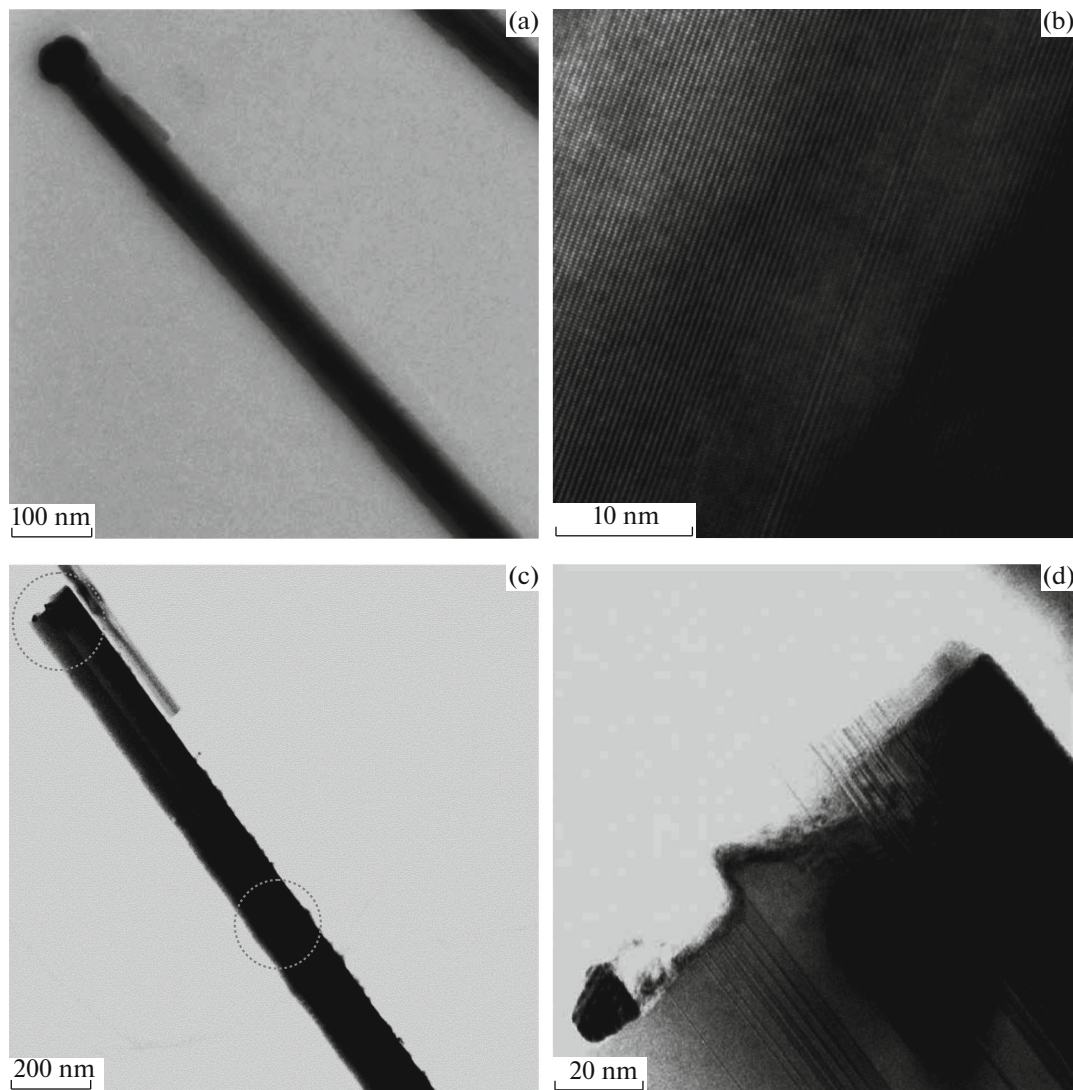


Fig. 2. (a) TEM image of a GaN NW, (b) magnified high-resolution TEM image of NW fragment, (c) transmission scanning electron microscopy image of an NT (circles indicate catalyst nanoparticles falling inside the tube), and (d) magnified high-resolution TEM image of the top part of the NT with a catalyst particle.

spectra of obtained nanostructures were measured, and the signal from NTs turned out to be more than 200 times as bright as that from NWs.

Acknowledgments. This study was supported in part by the St. Petersburg State University (project no. 11.37.2102016) and the Russian Foundation for Basic Research (projects nos. 17-52-51196 and 18-32-00942). TEM, CL, and EDX investigations were performed using instrumentation of the Interdisciplinary Resource Center (Nanotechnology Division) at St. Petersburg State University,

REFERENCES

1. J. W. Orton and C. T. Foxon, *Rep. Prog. Phys.* **61**, 1 (1998).
2. S. Zhao, A. T. Connie, M. H. T. Dastjerdi, X. H. Kong, Q. Wang, M. Djavid, S. Sadaf, X. D. Liu, I. Shih, H. Guo, and Z. Mi, *Sci. Rep.* **5**, 8332 (2015).
3. V. G. Dubrovskii, N. V. Sibirev, and G. E. Cirlin, *Tech. Phys. Lett.* **30**, 682 (2004).
4. S. Fernández-Garrido, V. M. Kaganer, K. K. Sabelfeld, T. Gotschke, J. Grandal, E. Calleja, L. Geelhaar, and O. Brandt, *Nano Lett.* **13**, 3274 (2013).
5. A. D. Bolshakov, A. M. Mozharov, G. A. Sapunov, I. V. Shtrom, N. V. Sibirev, V. V. Fedorov, E. V. Ubyivovk, M. Tchernycheva, G. E. Cirlin, and I. S. Mukhin, *Beilstein J. Nanotechnol.* **9**, 146 (2018).
6. V. Purushothaman and K. Jeganathan, *J. Nanopart. Res.* **15**, 1785 (2013).
7. Y. Zong, H. Huang, W. Song, R. Lv, D. Zhao, Z. Liu, Q. Guang, J. Guo, and Z. Tang, *Cryst. Res. Technol.* **51**, 757 (2016).

8. J. Yoo, Y.-J. Hong, S. J. An, G.-C. Yi, B. Chon, T. Joo, J.-W. Kim, and J.-S. Lee, *Appl. Phys. Lett.* **89**, 043124 (2006).
9. B. Monemar, *J. Phys.: Condens. Matter* **13**, 7011 (2001).
10. T. B. Wu and J. B. Cohen, *Acta Metall.* **31**, 1929 (1983).
11. K. A. Gschneider, Jr., R. W. Calderwood, H. Okamoto, and T. B. Massalski, in *Phase Diagrams of Binary Gold Alloys*, Ed. by H. Okamoto and T. B. Massalski (ASM Int., Materials Park, OH, 1987), p. 191.
12. X. Zhou, J. Chesin, S. Crawford, and S. Gradečak, *Nanotechnology* **23**, 285603 (2012).
13. X. Weng, R. A. Burke, and J. M. Redwing, *Nanotechnology* **20**, 085610 (2009).
14. F. Panciera, Y. C. Chou, M. C. Reuter, D. Zakharov, E. A. Stach, S. Hofmann, and F. M. Ross, *Nat. Mater.* **14**, 820 (2015).

Translated by P. Pozdeev